

Technical Design Report of Matsya 6A, Autonomous Underwater Vehicle

Akshat L., Mohan A., Sanjoli N., Vyankatesh S., Parth P., Piyush T., Nayan B., Aditya H., Shaunak N., Shubham T., Nandagopal V., Nakul R., Advait P., Sarat B., Rishabh D., Andrews V., Apurva K., Ruchir C., Vatsal S., Chaitanya T., Aditya G., Akshat Z., Nirmal S., Pranjal J., Sudarshan G., Vikram A., Devansh J., Sidharth M., Tejas B., Vignesh A., Aayush S., Ayushi G., Parvik D., Shiv M., Anagha S., Akash F., Ramyasri P., Sabhya S., Vinayak S., Mayur S., Hastyn D., Sarthak R., Raavi G., Kaustubh C., Rishabh R., Lyric K., Abhimanyu R., Advait R., Ammar B., Omkar P., Pratik S., Shivam A., Advaith S., Govind S., Kalp V., Sankalp B., Sankalp P., Abeer M., Sunandinee M., Sanya A., Nandini K., Aditya S.

Faculty Advisors: Prof. Leena Vachhani and Prof. Hemendra Arya

Abstract—Matsya is a series of Autonomous Underwater Vehicles (AUVs) being developed at the Indian Institute of Technology (IIT) Bombay to deliver a research platform in underwater robotics and promote autonomous systems. Significant architectural changes have been made to the subsystems by designing them to handle tasks in real-time. This year, the testing modes were also changed to accommodate the lack of a pool for in-water testing. Some of the key features include improved heat dissipation, the simulation of underwater localization system, and revamped controls and path planning. This paper presents an insight into the team's design process for the latest autonomous vehicle, *Matsya 6A*, and the analytical methods that the team used for the prototyping and development of the vehicle, including structural simulations, hydrodynamics analysis, underwater data transmission models, path controllers, and strategies to optimize the design.



Figure 1: Matsya 6A

I. COMPETITION STRATEGY

The objectives and challenges at RoboSub 2021 involve challenging environment manipulation. The approach towards the competition is to minimize errors and increase the vehicle's reliability in completing each task.

This year's target is the G-man and its related tasks, primarily because of its

well-characterized images having sharper contrast with the pool. Since Matsya has all the features required to try every task, attempts will be made to secure the maximum number of points in each task by attempting the highest scoring combination of tasks given the time constraints. Having encountered and completed the gate, pinger, buoy, and torpedo tasks in previous years, the team is confident about completing these tasks.

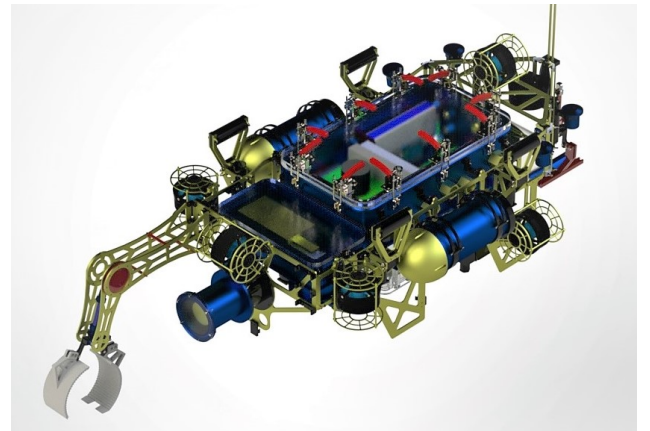


Figure 2: Computer-aided design (CAD) of Matsya 6A

During vacations, the team works around the clock to maximize the amount of time spent testing the vehicle in the pool. This year, the COVID-19 restrictions in India meant that the pool was inaccessible for testing, and hence the team spent the same time improving the simulation capabilities. The vehicle dynamics were better modeled in Gazebo. New Gazebo plugins were created to model waves in the simulator and generate bounding boxes for training the ML-based vision subsystem. A MATLAB and Simulink-based simulator with specialized utilities, enabling rapid prototyping of algorithms and models, was built to develop the controls, localization, and

motion planning capabilities.

Buckling analysis of all the hulls has been performed to ensure that they would not severely deform or collapse even upto the depth of 100m. Topology optimization has been implemented to reduce the weight of the components. It is an effective technique to optimize the structural design of the parts while maximizing the stiffness. Previously, the main hull of Matsya 5 was prone to heating issues, which at one instance even led to multiple electrical failures and forced the vehicle to shut down mid-run. This problem is addressed in Matsya 6A by developing heat dissipation mechanisms for the Graphics Processing Unit (GPU) and the Electronic Speed Controllers (ESCs), which are the primary sources of heat in the vehicle. Due to the absence of a pool for in-water testing, we designed an in-air waterproofing method. This involves detecting leakage points using an apparatus consisting of a pressure sensor, vacuum pump, and a safety valve.

The controls and navigation system have undergone a complete revamp to suit the RoboSub environment and the vehicle better. The single-input-single-output PID has been replaced by a multi-input-multi-output LQR Feedback based control structure. The allocation module and PWM mappings have been improved, and an Artificial Potential Fields (APF) based planner has replaced the previous breadth-first search-based implementation. Due to an increase in the number of parameters to tune, there was an urgent need to streamline the testing and debugging process, resulting in the introduction of multiple visual utility tools. These tools also enabled people unfamiliar with the software stack to run and debug the vehicle. To improve the performance in tasks requiring the arm, a modular arm has been developed with gripping feedbacks based on the current spikes when the object is grabbed.

Two vehicles will be simultaneously deployed - the Matsya 4A (M4A) and Matsya 6A (M6A) with a capacity-dependent distribution of tasks. This is an integral part of the team's strategy, as M4A will do the more straightforward tasks that do not require very accurate localization. Accurate localization is a challenge in M4A as it

lacks a Doppler Velocity Log (DVL) sensor. Presently, an approach using Extended Kalman Filter (EKF) based sensor fusion for localization is being explored to mitigate this problem.

The approach towards the pinger task was reworked entirely. The pinger localization algorithm has been modified to incorporate real-time ping detection and the processing has been shifted to the Field Programmable Gate Array (FPGA) to reduce the computational load on the CPU. This reduced the time spent on the pinger task to 150ms, which earlier collected data for 2-seconds and then look for a ping signal inside it.

II. VEHICLE DESIGN AND ANALYSIS

A. Mechanical Subsystem

The core philosophy behind the design of Matsya 6A is compactness, modularity, and reliability. The mechanical design can be bifurcated into Hulls and Frame (Structure and Component Positioning). A total of 8 thrusters have been used to provide active control of all 6 degrees of freedom to the vehicle. The vehicle is also equipped with various manipulation systems (Arm, Gripper, Torpedo Shooter, Marker Dropper). Any potential design undergoes an iterative procedure involving prototyping and critical design reviews until all design requirements are met. This design methodology is illustrated in Figure 3.

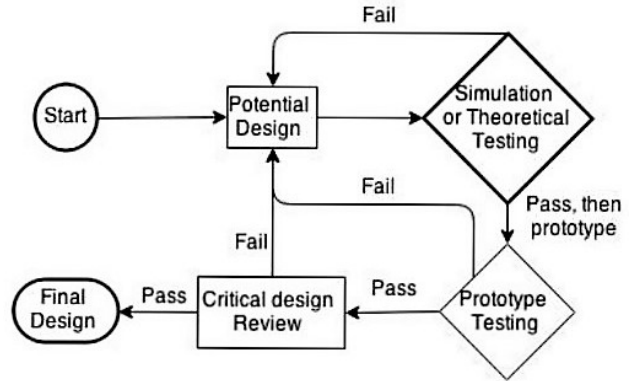


Figure 3: The potential design is first theoretically tested by running simulations followed by prototype testing and a critical design review (CDR) to qualify as the final design. Failure at any step results in re-designing the particular component.

The mechanical subsystem ensures the robustness of the design by running various analyses like structural, hydrodynamic, and

thermal studies of the vehicle. The following sections present the work on improving the structural integrity of hulls, drag reduction systems, thermal management solutions, and overall optimization of space and weight of the vehicle.

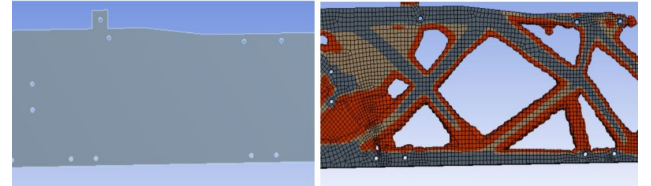
Structural Analysis: To ensure the vehicle's structural integrity, static structural and linear buckling analyses are performed.

Static Structural Analysis: The static structural analysis includes analyzing the hulls' stress, strain, and deformation under load using the Finite Element Analysis method. The strength of the hulls and frame of Matsya 6A has been tested by running simulations on ANSYS Static Structural. Furthermore, it is confirmed that the safety factor of all the pressure hulls and frame lies above 2 after applying the loads, pressure, and boundary conditions.

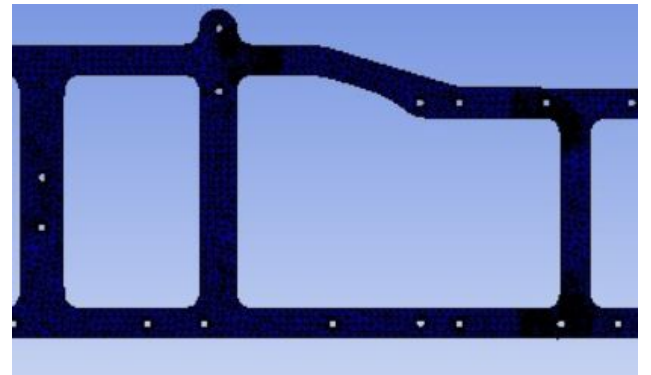
Linear Buckling Analysis: The Eigenvalue or LB Analysis predicts the theoretical buckling strength of an ideal linear elastic structure. Thus, linear buckling generally yields theoretical elastic buckling strength, not accounting for the imperfections and non-linear behaviors. It is performed on all the hulls, and critical buckling load is calculated through the load multiplier. The load is applied as a variable and iteratively analyzed to bring the load multiplier close to 1 and converge the load to the critical load. It is ensured that the vehicle's hulls would not severely deform or collapse at large depths through this study. Results show that none of the hulls will deform even up to 100m depth. Furthermore, the analysis leads to better insights on optimizing the thickness of the hull, the weight of the hull, and the need for support structures at critical points.

Topology Optimization: Topology optimization is an effective technique to optimize a structural design and minimize redundant material. The team's goal is to maximize the stiffness while reducing the weight of the components. The topology optimization has been performed by linking it with Static structural analysis on the frame of Matsya 6A. The frame is 5mm thick and is made up of Alloy Al-6061. Figure 4a shows a side view of the frame. The initial geometry provided the strength that was

more than necessary and had a very high safety factor. Therefore, the objective was to minimize compliance with a constraint to retain $\approx 50\%$ mass of structure in topology optimization analysis. Using the output obtained from optimization analysis, the previous design was modified, reducing mass by $\approx 48\%$ successfully. The safety factor has been verified to be greater than the threshold value by performing static structural analysis.



(a) Initial Geometry of the frame (left). Each hole in this frame corresponds to a mounting point and supports the load of different hulls or parts of the vehicle.; Optimised geometry as a result of topology optimization (right)



(b) Static structural analysis of final modified geometry.
Figure 4: Topology Optimization

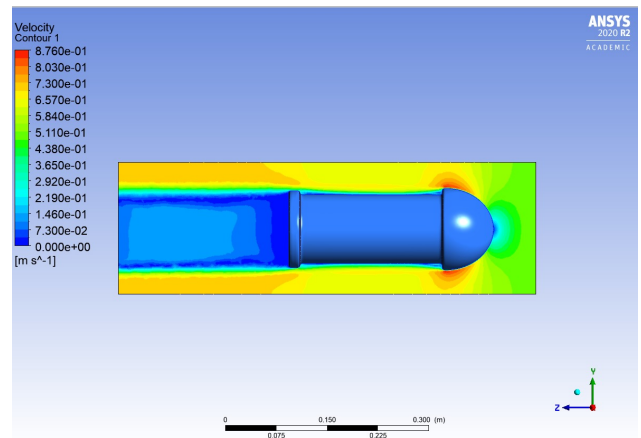


Figure 5: Velocity contours for the new battery hull attached with a dome-shaped structure to reduce drag. It is seen that there is a minimal high-pressure zone in the front, which would not be the case if the hull had a flat front face.

Hydrodynamic Analysis: The battery hull was forward covered with dome-like hydrodynamic structures to reduce the form drag. The hydrodynamic characteristics of the

axisymmetric battery hull were investigated to check the impact of the hydrodynamic dome placed in front of the battery hull. This increased the surge speed of the vehicle significantly due to the reduction in drag. The study was carried over the surge speed range of 0.25 to 1 m/s, and simulations were performed using the laminar models based on the finite volume method. The results were validated against values obtained by approximating C_d (drag coefficient) for appropriate geometries and Reynolds number (Re) to get the theoretical drag force. As a result, there is a 47% reduction in drag at the speed of 0.5 m/s, from 1.95 N (without dome) to ≈ 1 N (with dome).

Thermal Analysis: The primary heat-generating components in the Matsya 5 main hull were found to be the ESCs and the GPU. Innovative thermal management solutions were incorporated in Matsya 6A to tackle these components' heating issues.

ESCs control the flow of power to the thrusters. Since all the power used by thrusters passes through the ESCs, a large amount of heat is dissipated by them. To reduce the temperature in the main hull, the ESCs were moved to a separate hull. This ESC hull was designed to occupy minimal space and ensure good contact between the ESCs and the hull walls to dissipate heat effectively.

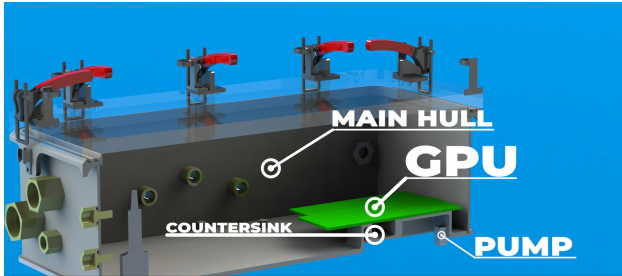
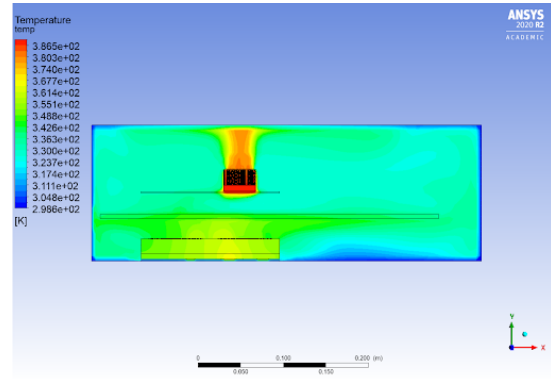


Figure 6: Section view of the main hull showing the GPU placed on the countersink with a pump just outside to circulate water near the countersink.

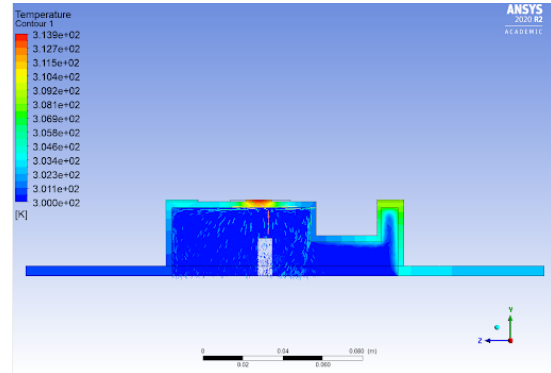
The heat-generating components inside the main hull include most of the electrical components, with the CPU and GPU generating most of the heat. CFD simulations were conducted to understand the temperature distribution and flow of heat in the hull. First, a CFD simulation of the Matsya 5 main hull was conducted. Figure 7a depicts the temperature contours of the main hull at the end of the simulation. Being the

biggest heat source, the GPU was the object in focus, and its peak temperatures were recorded to be as high as 95°C. This exceeds the operating temperature limits of the GPU. Thus, the GPU in Matsya 5 could not be operated to its maximum capacity. This issue was resolved in Matsya 6A by incorporating a new thermal management solution for the GPU, as shown in Figure 6.

CFD simulations of this novel thermal management system under maximum load were conducted to validate its performance, and the results obtained were very convincing. Figure 7b depicts the temperature contours of the GPU chip and the main hull baseplate at the end of this simulation. The system predicts a peak GPU temperature of 40°C, which is impressive compared to standard GPU thermal cooling solutions available off-market. Thus, the proposed thermal management solution is expected to ensure that the temperatures of the electronics in the main hull are well within their operating limits, thereby reducing the probability of failures.



(a) Temperature contours of the main hull with GPU and CPU with a plate separating modeling the electrical boards. Both the CPU chip and GPU chip have fans above them, pulling hot air out of the heatsink grooves.



(b) Temperature contours of Matsya 6A's thermal cooling solution under maximum load.

Figure 7: CFD simulations of the main hulls.

Sea State Analysis: A dynamic model for calculating forces on Matsya in sea-like conditions was devised to make the vehicle more robust to dynamic sea conditions. This force analysis is dynamic due to the depth-dependent, and time-varying velocity of the sea waves [1]. A velocity profile of up to 30m depth is deduced (Figure 8) by considering wind-generated waves and neglecting ocean currents and swells. Since a wind-generated wave can be seen as a superposition of a large number of regular waves, the Donelan Spectrum [2] is used for a variety of frequency ranges [3] to arrive at values of the velocity of sea waves at various depths. Using these velocity profiles, one can analyze the drag forces on the vehicle using its dependence on velocity v (usually $\propto v^2$). These drag forces can be used to develop control mechanisms that would make the vehicle more adaptive to non-ideal pool conditions [4].

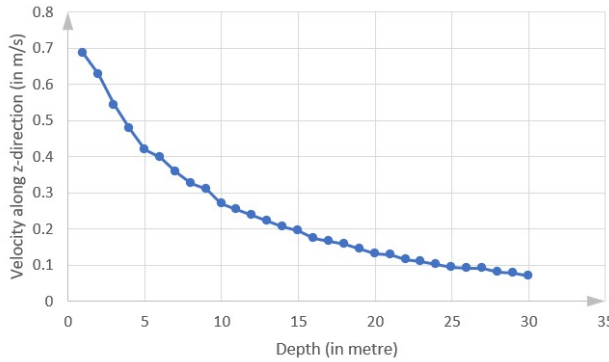


Figure 8: Velocity of the sea waves in z-direction (perpendicular to the sea surface) plotted against depth, up to 30 m. For a particular depth a summation of the 1000 values for every frequency is obtained and the phase angle is set randomly between 0 to 2π . This is done multiple times and Root Mean Squared (RMS) value is calculated.

B. Software Subsystem

The Software Stack of Matsya 6A has been developed on top of Robot Operating System (ROS). The software system is implemented as one stack with different packages representing various modules like vision, navigation, controls, firmware, and mission planning.

Design specifications of the stack ensure that it is extendable and generic. ROS helps in keeping the software modular with different tasks compartmentalized into various processes called nodes. ROS handles all the

Inter-Process Communication via messages and services. It is also generic enough to be plugged into other robotic frameworks. Figure 9 depicts the software architecture of Matsya 6A as described above.

A competition-like testing environment has been built on the Gazebo simulator which has the model of Matsya 6A and the tasks to test the different algorithms and heuristics for controls, state, vision, mission planning and acoustics.

The following sections present the work on software upgrades, implementing LQR-based optimal controller, Artificial Potential Field (APF) based path planner and path follower, dynamic modelling, logging system for restarting vehicle mid-run, optimal control allocation with thrust mappings and developments to streamline testing.

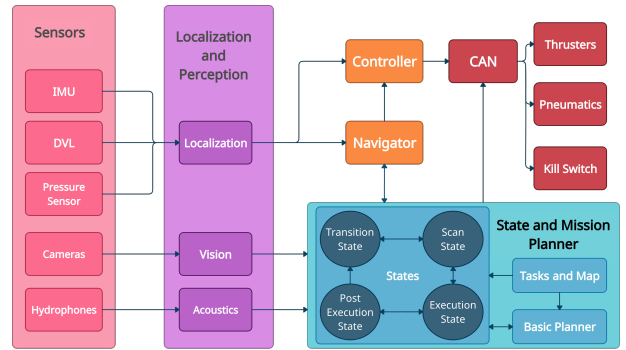


Figure 9: Software architecture of Matsya 6A depicting inter-package communication facilitated by ROS

Software Upgrade: The software stack has been upgraded from ROS Kinetic (EOL April 2021) to ROS Melodic (EOL May 2023).

Circle CI for Continuous Integration on GitHub has been set up in the project to handle compilation of our codebase with ROS Melodic on remote docker and to ensure LLVM Coding Standards for C++ and PEP 8 Style Guide for Python.

Linear Quadratic Regulator (LQR): Matsya's previous PID (Proportional Integral Derivative) based controller offered limited performance for our non-linear system. This year, an LQR-based optimal controller has been developed to improve performance and streamline the tuning and testing processes. The LQR controller is based on full state feedback and gives a choice to optimize for the state error or the controller input using the vehicle's dynamic model. This

model is computed in two matrices - the A and B matrices, on MATLAB. The A matrix represents the mechanical properties in the form of a symbolic state space, and the B matrix represents the control system details like the thruster orientations and configuration.

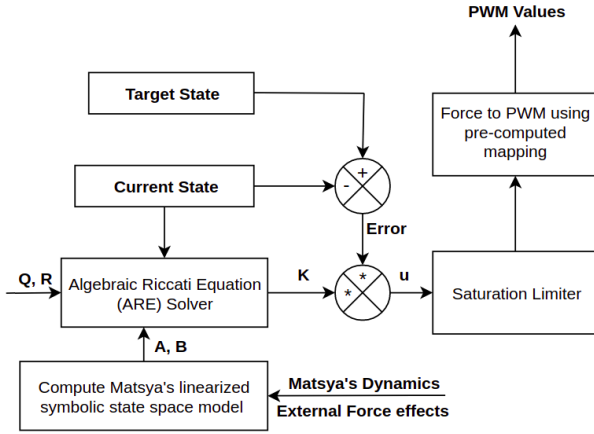


Figure 10: LQR Control System integrated into Matsya's codebase with Target State, Current State and Q , R (penalty matrices) as input, PWM Values for 8 thrusters as output

The model of the system also accounts for the drag, gravity, and Coriolis force. The Q and R matrices represent the state error and control input penalties, respectively. Finally, the A , B , Q , and R matrices are input to an iterative Discrete Algebraic Riccati Equation (DARE) Solver [5], which returns the gain matrix K [6], using which the optimal control inputs for Matsya's 6 DoFs are obtained. Finally, the allocation module optimally distributes these among Matsya's eight thrusters, prioritizing orientation control over translation. LQR has provided the ability to fine-tune controller performance while taking energy limitations into account.

Path Planner and Path Follower: A new path planning module based on the APF method has been developed in the navigator package [7]. A potential field is constructed by modelling obstacles and goal states as sources of positive and negative potential respectively. Figure 11 depicts a representative potential field for a task. The path is then computed by calculating gradients of this field. The module provides smooth obstacle-free paths without the requirement of maintaining an occupancy grid of the environment. Combined with the integrated and simulator-tested path follower, the vehicle is capable of efficient and robust

obstacle avoidance and navigation, with the help of the camera feed.

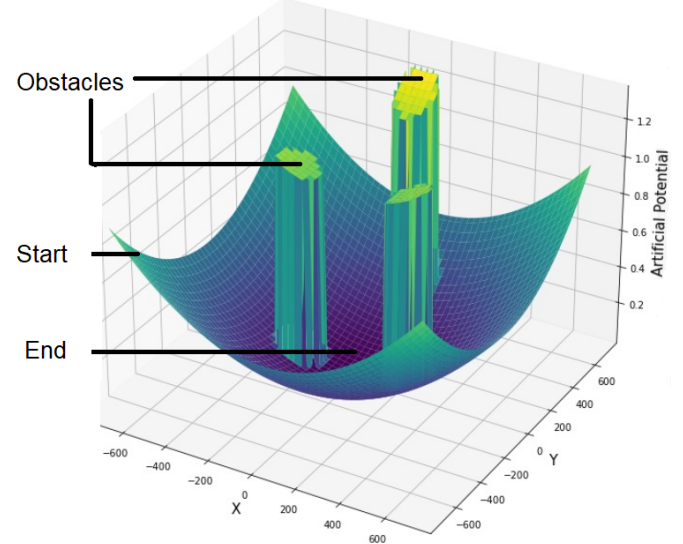


Figure 11: Generated Artificial Potential Field

Dynamics Modelling: The team attempted to improve Matsya's dynamic model. The model is based on the 6 DoF modelling framework given by T.I. Fossen [8]. Masses, moments of inertia, and location of the centre of gravity and buoyancy are obtained from the vehicle's CAD. Non-Linear Regression is applied on localization and propulsion data collected in step tests to estimate the drag and mass coefficients. These coefficients have aided in the further development of our simulator, controls and localization which rely on an accurate dynamic model

Restarting the vehicle: A data logging system has been implemented to ensure that Matsya can autonomously resume operation post an unexpected shutdown. This system stores all the essential information, such as the task currently in execution and the vehicle's position in YAML files. Upon start-up, these logs are checked for data, the lack of which signifies that the run was successfully completed. If the log files contain data, they are parsed and processed, and Matsya is updated with the vital guidelines to resume from the point where it stopped.

Optimal Control Allocation and Thrust Mapping: A new optimal allocator based on inverse kinematics has been developed. It uses the pseudo-inverse of the control matrix [9] which minimizes the

least-squares error between desired and available control inputs. A new thrust-PWM mapping using piece-wise polynomials was developed and tuned using the thruster's data. Together the thruster outputs can be allocated more precisely and efficiently for a broader range of thruster configurations.

Developments to streamline testing:

A significant portion of the team's time is spent on testing the vehicle. As the codebase has been in development for nine years, the number of parameters necessitates visual aids. A terminal utility has been developed that elegantly presents all the necessary information ranging from battery and sensor status to task success, all in a single window. This GUI removes the need to monitor multiple terminal windows constantly, thus simplifying the debugging process. Similarly, the PID Tuning process has been streamlined by introducing a tuning and testing GUI, which also plots the localization data in a single window. Figure 12 depicts a representative image of the developed GUI.

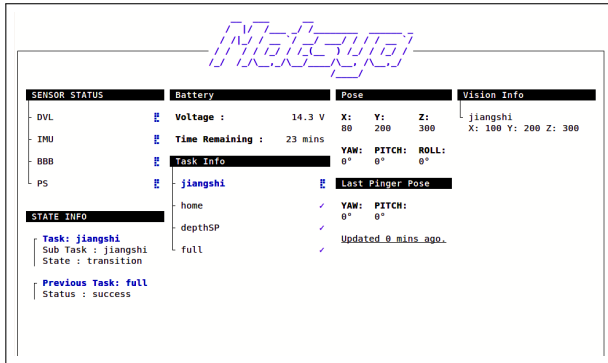


Figure 12: Terminal Utility Display

C. Electrical Subsystem

One of the primary requirements of the vehicle is power distribution across the components of the vehicle. The communication between components, speed of the thrusters, the pneumatic systems are all controlled by the Electrical Stack. The stack is further divided into electrical boards, on-board computer, GPU, ESCs and supporting circuits.

Figure 14 depicts a flowchart of the electronics architecture. The electrical stack is made to be modular to ensure the ease of assembly and wiring.

ESC Hull: The ESC hull comprises a custom-made power distribution box for eliminating the wire clutter in the main hull. A mechanical Latch Relay is deployed to sever the connection to the battery in case of vehicle failure. A system is built to monitor the PWM signals given to each ESC.

Electrical Stack: The main electrical stack of Matsya 6A is equipped with many features that offer controlled redundancy and debug capabilities to mitigate in-run failures.

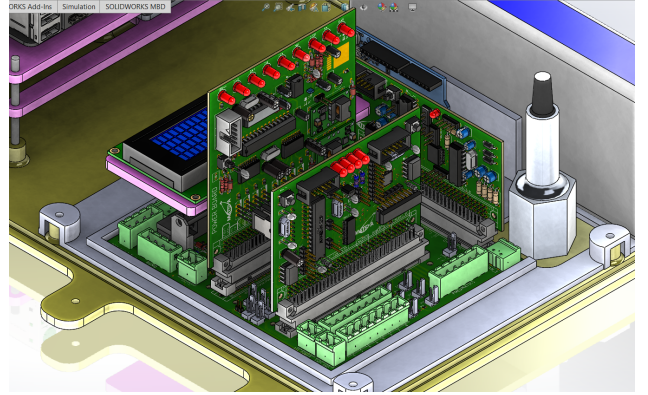


Figure 13: The Electrical Stack of Matsya 6A comprises the Backplane, GPIO, Power and Debug boards (located at the bottom, front, back and right respectively)

The Debug board: This board captures data from all the sensors on-board, the electrical stack and PWM channels. It also logs data in an SD card for later analysis. This data is also sent to the motherboard for real-time decision-making. We also have Status LEDs to get visual feedback about the vehicle state (scanning, transition, or execution) during an autonomous run. This time, a new full-size LCD panel displaying currents, voltages, and temperature readings by communicating with the motherboard was added, making debugging faster and more efficient than ever before.

The GPIO board: This board has two different micro-controllers capable of controlling the entire vehicle independently, ensuring dual redundancy and user-selected complexity. In addition, the Debug Board and the GPIO facilitate mutual feedback and restores the system in case of any micro-controller failures.

The Power board: This board generates and supplies all the different voltage levels required for all the sensors, other electrical circuit boards, and the motherboard. The board also houses eight mutually exclusive

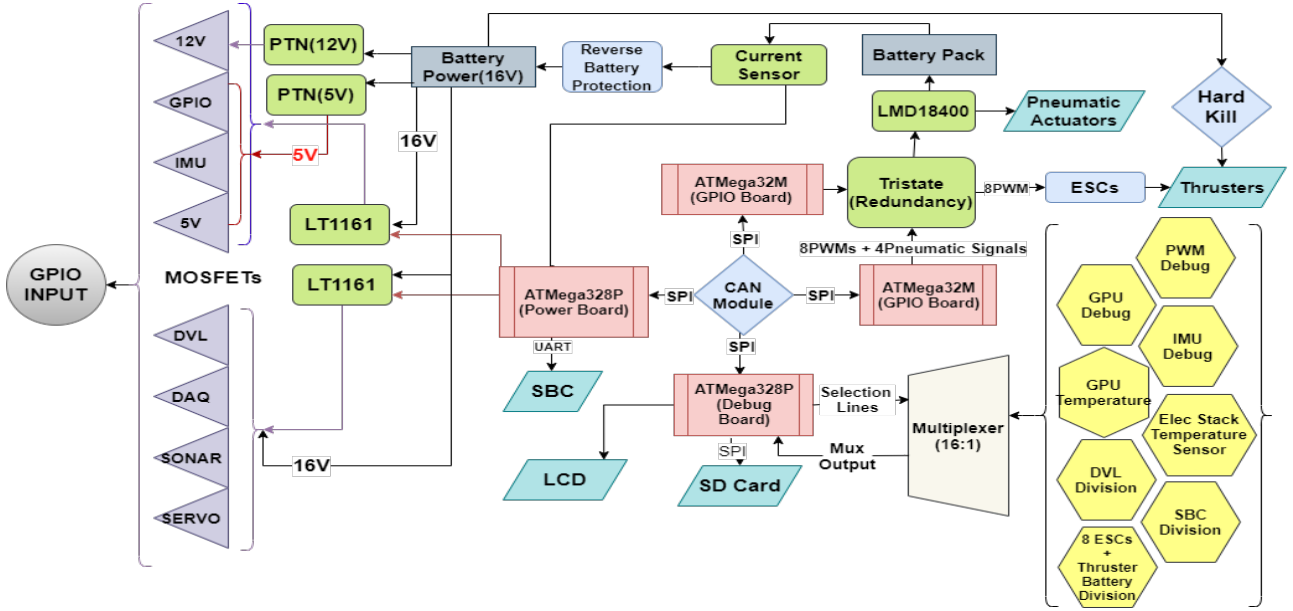


Figure 14: Electrical architectural diagram exhibiting the internal communication and power distribution

toggle lines to better control the power across the vehicle with additional features like reverse battery and over-voltage protection.

The Backplane: This board houses the Power, GPIO, and Debug boards and ensures easy connections and routing to all the other peripherals and sensors. In addition, the Backplane provides one-point interfacing of the electrical stack with the sensors and the motherboard.

A new Motherboard - Gigabyte B450I was used this time, which houses the AMD Ryzen 3400G processor. The mini-ITX form factor ensures a compactness and has all the peripherals sockets required for the connections. The TMP236x temperature sensors were introduced to regions prone to high operating temperatures to monitor these regions effectively. LED strips were installed at the top of the main hull to indicate the current status of the task which the vehicle is performing. The BlueROV leak sensors monitor any potential water leakages inside the main hull.

Underwater Acoustic localization Model: One of the competition tasks includes determining the acoustic wave source or pinger position in the swimming pool. Since in-water testing is not possible due to COVID-19 restrictions, a digital model of a pinger and an underwater channel [10] was created to simulate the pinger task. The channel is capable of manipulating and

propagating the digitally generated acoustic waves of the pinger [11], [12].

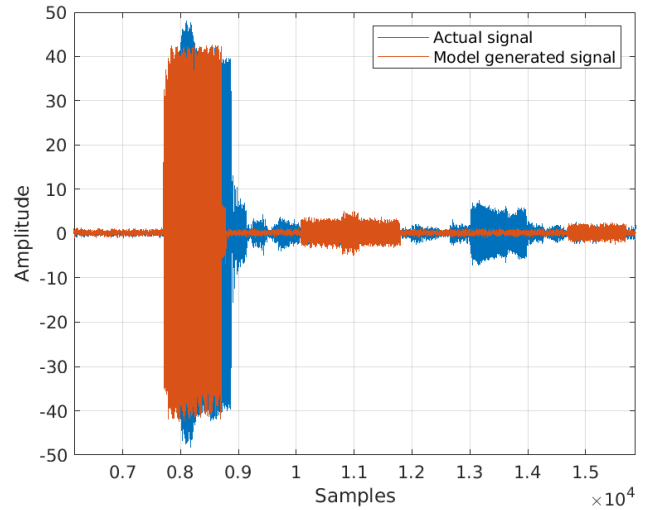


Figure 15: Actual Data sampled from the Teledyne RESON TC4013 Hydrophone after signal propagation through water v/s Data generated by the MATLAB model

A mathematical model of the pinger was created in MATLAB, which generates the ping signal of the desired frequency. A rectangular swimming pool was also simulated to propagate this wave, considering attenuation, reflection, and underwater channel noise[13], [14], [15]. Finally, using this model, the data was generated and sampled by the array of four hydrophones. This data resembled the actual hydrophones' data collected in the pool, which helped us refine the pinger localization scheme

incorporating real-time ping detection. The newer algorithm computes the Time Difference of Arrival (TDOA) [16] in 150 ms, faster than the earlier model that collected data for 2 seconds.

Localization of underwater sources using FPGAs: The project aimed to replace the Data Acquisition system (DAQ) in the vehicle using hardware that supports faster processing speeds. Xilinx ZC7020 Field Programmable Gate Array (FPGA) was used to implement the localization algorithm based on TDOA[16]. Performance improvement and size reduction were the primary objectives of this project.

The initial implementation of the TDOA algorithm in software was used to utilize all the CPU cores of the Intel processor in the motherboard. In contrast, this functionality has now been transferred to the FPGA, increasing the efficiency, decreasing the processing time and reducing the load on the motherboard. The algorithm flowchart is synthesized using Xilinx Vivado 2019.1 Design tools. The model data generated from the Underwater Acoustics Model Project was used to validate the implementation for simulation purposes.

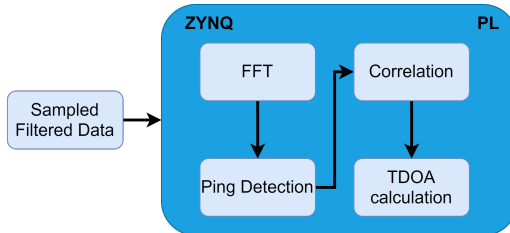


Figure 16: Block Diagram of Static Localization using FPGA

Upgrading to ARM-based architecture: With the electrical stack becoming increasingly complex with each vehicle, we sought to upgrade it. To keep up with the industrial practices, ARM and PIC-based micro-controllers were explored to replace the current AVR-based micro-controllers due to the superiority in power consumption, processing speed, and the number of available GPIO pins, among other things. After careful consideration, taking into account the compatibility of previously used sensors regarding the communication protocols, voltage compatibility, the ARM microcontrollers were chosen. The final choice

was the STM32G4 series microcontroller from STMicroelectronics that proved to be cost-effective and also has an inbuilt Controller Area Network (CAN) module that eliminates the need for CAN transceiver ICs like the MCP2561 and MCP2515.

Battery Management System: Matsya uses two 4S LiPo batteries having the capacity of 16000 mAh for powering the thrusters, microcontrollers and other components in the vehicle. Therefore, it is necessary to keep track of the battery performance and the operational time while checking for malfunctions. Once a fault has been detected, it needs to be resolved on a priority basis while maintaining the vehicle's functioning during the run. For this purpose, we have developed a Battery Management System[17] consisting of the Skycell LiPo batteries, a pack of 4 individual cells connected to the BMS board through MOSFET switches. The BMS board measures the discharging current of a battery and integrates the discharging current over time to estimate the State of Charge [18]. This method of State of Charge estimation is called the Coulomb Counting[19]. Also, the BMS board measures the temperature and the voltage of the battery cells. Passive cell balancing is implemented using LTC6804 by monitoring multiple cells configured using external MOSFETs.

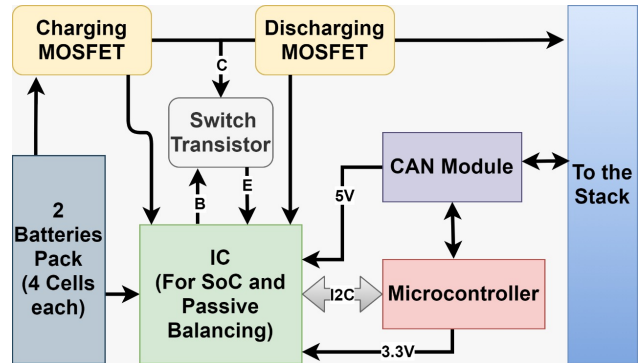


Figure 17: Battery Merging System Implementation

Passive Cell Balancing allows batteries to have a uniform State of Charge (SoC) by dissipating the power of higher State of Charge cells through MOSFETs [20]. This has enabled us to maintain individual cell voltage levels and balance charge the batteries without removing them from the battery hull. The BMS system helps estimate operational run-time calculation, keeps a check on battery

performance, reduces the fear of battery over-utilization.

III. EXPERIMENTAL RESULTS

In-water testing was entirely restricted due to the country's lockdown protocols, but the same time was utilized to make significant improvements to the simulator. To train the ML-based vision subsystem, a gazebo plugin was implemented that can automatically detect tasks in the camera feeds and draw bounding boxes around them. It has saved countless hours over the previously manual labeling process. To better model the underwater conditions and test the rigidity of our controls subsystem, underwater current plugins for Gazebo were created. Taking this a step further, waves modeled based on the Pierson-Moskowitz Spectrum have been incorporated [1]. It has enabled more rigorous testing of the controller by simulating waves as a disturbance.

The pinger task rework was a great success. We created a full-fledged MATLAB model to characterize the pinger, pool, hydrophones and include all underwater effects on acoustic signals. The older algorithm took 2 secs to collect the data and then process it to find the ping signal, whereas the refined algorithm takes only 150ms with real-time ping detection to make the system more efficient.

With a lack of in-water testing, a mechanism was devised by the mechanical subsystem of the team to ensure the waterproofing of the hulls that house the electronics in them. This technique is called in-air waterproofing.

In-air waterproofing involves detecting leakage points by recreating the actual pressure conditions faced by the vehicle underwater using a vacuum pump. The pressure readings are processed from the hull using a pressure sensor without going to a pool. It is inferred that the time constant in the pressure plot (pressure readings from the sensor vs. time) is proportional to the diameter of the potential leakage point through a systematic set of experiments. This elegant approach proved to be a remarkable preliminary test to detect fault points early, thereby saving a lot of effort and time compared to the conventional in-water testing

approaches used for the previous iterations of Matsya.

Apart from this, the same equipment can pressurize the hulls to equalize the internal and external pressure conditions for any operating depth. Reducing the difference in pressure between the inside and outside of the hull reduces the chances of water seepage.

Furthermore, ISO 3601 certified industrial standards are followed that decrease the chances of O'ring failure caused due to alignment mismatch between groove dimension and O'ring[21].

IV. CONCLUSION

Despite having to work remotely, all the subdivisions of the team worked in harmony to create Matsya 6A by doing in-depth analysis to create a robust design and finally test it in the simulator. Matsya 6A is the most advanced vehicle the team has made and can quickly adapt and incorporate additional features without significant developmental changes. The lack of a pool for in-water testing was not felt, as the team's philosophy of working with what we have came to the fore, with significant changes made to the testing methods across the team, from using in-air waterproofing to incorporating terminal utilities for smoother simulations. Matsya 6A acts as an excellent launchpad for the team to further pursue its research in Underwater and Autonomous Robotics.

V. ACKNOWLEDGEMENTS

The team would like to thank the Industrial Research and Consultancy Centre of IIT Bombay for administrative and monetary support during the project and for helping us participate in RoboSub 2021. The support of the Dean R&D's office was crucial in the successful execution of the project. We would also like to thank Prof. PSV Nataraj from SysCon, IITB, for issuing us a GPU on which we could train our Machine Learning Models.

REFERENCES

- [1] "Waves: Wave Spectra." <https://www.orcina.com/webhelp/OrcaFlex/Content/html/Waves,Wavespectra.htm>. Accessed: 2021-04-10.
- [2] M. A. Donelan, J. Hamilton, and W. Hui, "Directional spectra of wind-generated ocean waves," *Philosophical Transactions of the Royal Society of London. Series A, Mathematical and Physical Sciences*, vol. 315, no. 1534, pp. 509–562, 1985.
- [3] "Ocean-Wave-Spectra." https://wikiwaves.org/Ocean-Wave_Spectra#JONSWAP_Spectrum. Accessed: 2021-04-10.
- [4] M. A. Nair and V. S. Kumar, "Wave spectral shapes in the coastal waters based on measured data off karwar on the western coast of india," *Ocean Science*, vol. 13, no. 3, pp. 365–378, 2017.
- [5] "Riccati Solver." https://github.com/TakaHoribe/Riccati_Solver. Accessed: 2020-10-17.
- [6] S. B. Bae, D. H. Shin, S. T. Kwon, and M. G. Joo, "An LQR controller for Autonomous Underwater Vehicle," *Journal of Institute of Control, Robotics and Systems*, vol. 20, no. 2, pp. 132–137, 2014.
- [7] K. M. Lynch and F. C. Park, "Motion Planning," in *Modern Robotics: Mechanics, Planning, and Control*, ch. 10, pp. 388–394, Cambridge University Press, 2017.
- [8] T. I. Fossen, "Models for Ships, Offshore Structures and Underwater Vehicles," in *Handbook of marine craft hydrodynamics and motion control*, ch. 7, pp. 167–183, John Wiley & Sons, 2011.
- [9] T. I. Fossen, "Motion Control Systems," in *Handbook of Marine Craft Hydrodynamics and Motion Control*, ch. 12, pp. 398–411, John Wiley & Sons, 2011.
- [10] X. Wang, X. Wang, R. Jiang, W. Wang, Q. Chen, and X. Wang, "Channel Modelling and Estimation for Shallow Underwater Acoustic OFDM Communication via Simulation Platform," *Applied Sciences*, vol. 9, no. 3, 2019.
- [11] S. Gul, S. S. H. Zaidi, R. Khan, and A. B. Wala, "Underwater Acoustic Channel Modelling using BELLHOP Ray Tracing Method," in *2017 14th International Bhurban Conference on Applied Sciences and Technology (IBCAST)*, pp. 665–670, 2017.
- [12] L. Emokpae and M. Younis, "Surface based underwater communications," in *2010 IEEE Global Telecommunications Conference GLOBECOM 2010*, pp. 1–6, IEEE, 2010.
- [13] G. Burrowes and J. Y. Khan, "Short-range underwater acoustic communication networks," *Autonomous Underwater Vehicles*, pp. 173–198, 2011.
- [14] Y. Y. Al-Aboosi, M. S. Ahmed, N. S. M. Shah, and N. H. H. Khamis, "Study of absorption loss effects on acoustic wave propagation in shallow water using different empirical models," *Journal of Engineering and Applied Sciences*, 2017.
- [15] T. Melodia, H. Kulhandjian, L.-C. Kuo, E. Demirors, S. Basagni, M. Conti, S. Giordano, and I. Stojmenovic, "Advances in Underwater Acoustic Networking." <https://doi.org/10.1002/9781118511305.ch23>, 2013.
- [16] O. Le Bot, J. I. Mars, C. Gervaise, and Y. Simard, "Cross recurrence plot analysis based method for tdoa estimation of underwater acoustic signals," in *2015 IEEE 6th International Workshop on Computational Advances in Multi-Sensor Adaptive Processing (CAMSAP)*, pp. 1–4, IEEE, 2015.
- [17] C. S. Chin, J. Jia, J. Chiew, W. Toh, Z. Gao, C. Zhang, and J. McCann, "System design of underwater battery power system for marine and offshore industry," *Journal of Energy Storage*, vol. 21, pp. 724–740, 02 2019.
- [18] H. Rahimi-Eichi, F. Baronti, and M.-Y. Chow, "Online Adaptive Parameter Identification and State-of-Charge Coestimation for Lithium-Polymer Battery Cells," *IEEE Transactions on Industrial Electronics*, vol. 61, no. 4, pp. 2053–2061, 2013.
- [19] I. Baccouche, S. Jemmali, A. Mlayah, B. Manai, and N. E. B. Amara, "Implementation of an improved Coulomb-counting algorithm based on a piecewise SOC-OCV relationship for SOC estimation of li-IonBattery," *arXiv preprint arXiv:1803.10654*, 2018.
- [20] R. Hu, "Battery management system for electric vehicle applications," 2011.
- [21] P. Seals, "Parker O-Ring Handbook (ORD 5700)," *Parker Seal Group, Lexington, KY*, 1992.

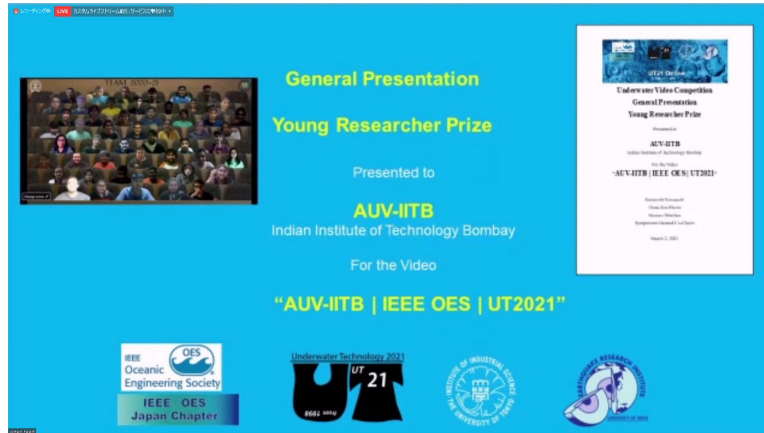
APPENDIX A: COMPONENT SPECIFICATIONS

Component	Vendor	Model/Type	Specs	Cost (new)	Status
Bouyancy Control	Designed In-House	Dead Weights & Foam	-	-	Installed
Frame	Designed In-House	Aluminium & Delrin	4 kg	800 USD	Installed
Waterproof Housing	Designed In-House	Aluminium Hulls w/ Acrylic Endcap	8 Hulls weighing 22 kg Depth Rating : 70 ft	2100 USD	Installed
Waterproof Connectors	Designed In-House	Aluminium	24 connectors weighing 1.5 kg in total	150 USD	Installed
Thruster	Blue Robotics	T200	11 and 9.5 kgf forward and backwards	1600 USD	Installed
Motor Control	Blue Robotics	Basic Version R3	30A PWM controlled brushless motor speed controller	200 USD	Installed
High Level Control	Microchip Technology	Atmega 328P and 32M	Low Power CMOS 8-bit RISC Microcontrollers	15 USD	Installed
Actuators	Janatics	A51012025O	Stroke Length: 25mm	30 USD	Installed
Battery	SkyCell	LiPo Battery	4 Cell and 16000mAh x 2	400 USD	Installed
Converter	Texas Instruments	PTN 78060	6A wide input output Adjustable switching regulator	50 USD	Installed
FPGA	Xilinx	Zybo Z7-20	Programmable logic equivalent to Artix-7 FGPA, DDR3L memory controller with 8 DMA channels and 4 High Performance AXI3 Slave ports, 667 MHz dual-core Cortex-A9 processor	300 USD	Installed
Regulator	Mini-Box	M4ATX	High efficiency 250W output, < 1.25mA standby current	80 USD	Installed
CPU	AMD	Ryzen 3400G (4C8T)	4 Cores (4.2GHz), 8GB RAM	-	Selected
GPU	Nvidia	GeForce GTX 1660ti	GDDR5, 6GB, 120W	300 USD	Installed
Internal Comm Network	Microchip Technology, CAN USB	MCP 2515, MCP 2551, CAN USB	1 MB's operation limit	150 USD	Installed

External Comm Interface	-	Ethernet	10-100 Mb/s	-	Installed
Inertial Measurement Unit (IMU)	Microstrain	GX5	-	-	Selected
Doppler Velocity Log (DVL)	Teledyne	Explorer DVL	-	-	Installed
Camera(s)	Allied Vision	MakoG-243	-	-	Installed
Hydrophones	Teledyne	RESON Underwater TC 4013	-	-	Installed
Manipulator	Designed In-House	-	1 DOF servo-operated arm, pneumatic driven end-effector	300 - 350 USD	Installed
Algorithms: Vision	YOLO v3	-	Parallel and Sequential processing, lens formula	-	Implemented
Algorithms: Acoustics	FFTW	Time difference of arrival	Filtering in frequency & time domain	-	Implemented
Algorithms: Localization and Mapping	Orcos BFL	Extended Kalman Filter	EKF applied on position found by integration of DVL velocity	-	Implemented
Algorithms: Autonomy	-	State Machine & Mission Planner	Probabilistic (or Finite) state machine for mission planner, designed in-house	-	Implemented
Open Source Software	OpenCV, Eigen, ROS, YOLO v3	-	-	-	Implemented
Team size	55	-	-	-	-
HW/SW expertise ratio	2:1	-	-	-	-
Testing time: simulation	250 hrs	-	-	-	-
Testing time: in-water	0 hrs	-	-	-	-
Inter-vehicle Communication	-	-	-	-	-
Programming Languages	C++, Python	-	-	-	-

APPENDIX B: OUTREACH ACTIVITIES

Team AUV-IITB is the recipient of the prestigious Young Researchers' Prize awarded by IEEE OES (Ocean Engineering Society) at Underwater Technology Competition 2021, organized by the University of Tokyo, Japan. We presented a 15-minute long video highlighting our journey so far, including the development of six underwater vehicles and various research projects the team has undertaken over the years.



Team AUV-IITB presenting at Video competition organised by University of Tokyo, Japan

The research and development of Matsya 6A got featured in Janes - an international level defense-related magazine. AUV-IITB is amongst the first student teams from India to be recognized at this level.

Team AUV-IITB participated in the Engineer's Conclave as a part of the contingent of IIT Bombay at the inter-IIT Tech Meet 2021 held virtually. The team presented a poster demonstrating the working methodology and capabilities of Matsya. The event helped in increasing the team's outreach amongst like-minded tech enthusiasts coming from various IITs. The progress made by the team was acknowledged and appreciated by all the participants.

Last year, the team participated in the Tech Expo event of Abhiyantri 2020, the Annual Technical Festival of KJ Somaiya College of Engineering, Mumbai. The team presented the history of Matsya from 2011 to 2020 to a large number of technocrats, enthusiasts, and students. This expo had exhibits from major organizations like DRDO, BARC, IMD, and DAE.

We also participated in MTS TECHSYM-2020's Students' Technical Symposium On Advances In Engineering and Technology, held at IIT Madras, where we interacted with professors and students from all across the country working on various maritime technologies. We presented a poster highlighting the various advances made in Matsya with the hope of encouraging other AUV teams along their journey. We received a special mention for the same.

Team AUV-IITB was invited to present a research paper for the prestigious International Conference INEST India 2020, INS Shivaji, Lonavala before the Chief of Navy and International marine specialists. Unfortunately, the event was called off due to Covid-realated circumstances.

The research that was done by the team also helped several students in their Masters/BTech projects on topics like Control of Overactuated Nonlinear Systems, Navigation of Unmanned Vehicles, Design of a 2-Link gripping mechanism, and Sunlight flicker removal. This further fuels the team to work harder and deliver results.

The team also mentors quite a few other teams from India keen on making AUVs, like IEM Kolkata, KJ Somaiya College of Engineering, Mumbai, Sahyadri College, NIT Rourkela, IIT Kanpur, and VIT Pune. The team guides them through the overall procedure of making an AUV, the importance of communication and documentation, and the process of acquiring funds for making AUVs in their respective colleges.